



ERNEST ORLANDO LAWRENCE BERKELEY NATIONAL LABORATORY

Control of Longitudinal Collective Behavior in the Muon Collider Rings

Wen-Hao Cheng, Andrew M. Sessler,
William C. Turner, and Jonathan S. Wurtele

Accelerator and Fusion
Research Division

May 1997

Presented at the
*1997 Particle
Accelerator
Conference*,
Vancouver, B.C., Canada,
May 12–16, 1997,
and to be published in
the Proceedings

LOAN COPY
Circulates
For 4 weeks
B1g. 50 Lib Rm 4014
Lawrence Berkeley National Laboratory

Control of Longitudinal Collective Behavior in the Muon Collider Rings*

Wen-Hao Cheng¹,
Andrew M. Sessler², William C. Turner²,
and Jonathan S. Wurtele^{1,2}

¹Department of Physics, University of California
Berkeley, California 94720 USA

²Ernest Orlando Lawrence Berkeley National Laboratory
Berkeley, CA 94720 USA

May 1997

* This work was supported by the Director, Office of Energy Research, Office of High Energy and Nuclear Physics, Division of High Energy Physics, of the U.S. Department of Energy under Contracts No. DE-AC 03-76SF00098 and DE-FG 03-95ER40936.

CONTROL OF LONGITUDINAL COLLECTIVE BEHAVIOR IN THE MUON COLLIDER RINGS *

Wen-Hao Cheng, Andrew M. Sessler, William C. Turner, and Jonathan S. Wurtele
Lawrence Berkeley Laboratory
Berkeley, California 94720

Abstract

The longitudinal single bunch collective effects in a Muon Collider [1] ring are theoretically examined. The situation involves an intense bunch, a short bunch, a small momentum compaction, a rather large impedance compared with the stability threshold criterion, and a luminosity life time limited by muon decay to a thousand turns. Qualitative descriptions of stability are given and a scaling law for the instability threshold is derived. Numerical simulation results for the impedance-related instabilities are given for two cases of current interest - a 250 GeV \times 250 GeV demonstration machine and a 2 TeV \times 2 TeV high energy machine. The results of these simulations are in good agreement with the predictions of the scaling law and show that the longitudinal collective effects are controllable with a proper choice of parameters (viz. rf voltage, rf frequency, linear and non-linear longitudinal chromaticity).

1 LONGITUDINAL BEHAVIOR

A ring with a high degree of isochronicity (i.e. a small slippage factor $|\eta| = |pdC/Cdp - 1/\gamma^2| = 10^{-7} \sim 10^{-5}$, where $\gamma = 1/\sqrt{1 - \beta^2}$, p is the particle momentum, and C is the circumference of the ring) is needed to satisfy the requirement of a short bunch with a practical rf system [1]. However, small $|\eta|$ implies small longitudinal Landau damping. Small $|\eta|$ also implies that the static effect of the longitudinal wake force causing potential-well distortion of a beam is important. The longitudinal motion of the beam is one of the main concerns for a muon collider ring [2].

A large number of accelerator parameters enter into the description of longitudinal beam motion. Although each of these impacts the analysis of beam stability, the values of many of them are fixed by considerations that do not involve beam stability, and they are not available for manipulation to improve the beam stability situation. Some examples of the fixed parameters are: beam energy, circumference, peak beam current, bunch length, momentum spread etc.. However, there remain a few free parameters that can be adjusted for longitudinal beam stability. They are: the lowest order and higher orders of the slippage factor, i.e., η_1, η_2, η_3 ; the supply of rf energy per turn, eV_{rf} ; and the wavelength of rf, λ_{rf} . Here, the slippage factor is expanded as $\eta = \eta_1 + \eta_2\delta + \eta_3\delta^2$, where $\delta = dp/p$. In this study, we use multi-particle simulations [3] to search

for a workable operation region in the parameter space: $\pm\eta_1, \eta_2, \eta_3, (V_{rf}/\lambda_{rf})$. A key ingredient in these analyses is the choice of broad-band impedance model to describe the electrodynamic interaction of the beam with beam tube discontinuities. In this paper, we use a broad-band ($Q = 1$) resonator model [4]. The ring inductance and resonant frequency of the model are chosen by scaling [5] from the impedance budgets (inductance and loss factor) that have been reported for B factories (PEPII and KEKB). The scaling takes account of differences in circumference, beam tube radius and bunch length and yields an impedance that is representative of the state of the art for smooth beam tubes. To fit the impedance of existing machines scaled to the muon collider rings, we use the parameters of the broad-band resonator model: shunt impedance $R_s(k\Omega) = 18.8$ (2 TeV), $3.1(250\text{GeV})$; $Q = 1$; and the resonant angular frequency $\omega_r = 17\text{GHz}$ for both rings. The low frequency broad-band impedance of the rings is $|Z_0^{\parallel}/n| = \omega_0 L = 0.26\Omega$, where ω_0 is the revolution angular frequency and L is the ring inductance. The rf cavity impedance is also included in our simulations. We use Perry Wilson's scaling formula for the longitudinal wake function [6]. Effects of Landau damping, potential-well distortion, nonlinear synchrotron oscillation, longitudinal microwave instability, and also, intensity decrease due to mu-decay, are all included in the simulations. Since the muon storage time is typically only a thousand turns, the system is in a transient state. The choice of storage ring working point will be seen to depend on the tolerance for bunch lengthening and energy spreading during the storage time.

1.1 How isochronous? The value of $|\eta_1|$.

Simulations show that the most suitable values of $|\eta_1^{\mu}|$ (when $\eta_2 = \eta_3 = 0$) are: $\sim 10^{-6}$ for the 2 TeV machine and $\sim 10^{-5}$ for the 250 GeV machine, which for reasonable rf voltage gives tolerable bunch centroid drift, energy spread growth, and bunch lengthening, compared to smaller η_1 . This is simply because larger $|\eta_1|$ gives faster Landau damping, where the Landau damping rate can be approximated as $\tau_d^{-1} = n\sigma_{\omega} = n\eta_1\omega_0\sigma_{\delta}$ [7]. Our simulations show that, the regime of $|\eta_1| \leq |\eta_1^{\mu}|$ freezes the z -motion but engenders in the δ -motion a correlated growth of σ_{δ} which quickly exceeds the lattice momentum acceptance. The regime of $|\eta_1| \simeq |\eta_1^{\mu}|$ smears the wake field-energy correlation and reduces the growth of momentum spread and bunch lengthening. Increasing η_1 further to $|\eta_1| > |\eta_1^{\mu}|$ results in unreasonably large rf voltage (to match the phase

* Work supported by the U.S. Department of Energy under contract No. DE-FG03-95ER40936 and DE-AC03-76SF00098

space) for acceptable bunch length and momentum spread.

1.2 How much rf? The value of V_{rf}/λ_{rf} .

Since increasing the rf gradient results in improved compensation of the variation of wake potential across the bunch, the problem of longitudinal behavior in the muon collider rings can be ameliorated by employing a large V_{rf}/λ_{rf} . Furthermore, for a given V_{rf}/λ_{rf} , the value of V_{rf} will be reduced by using a high rf frequency. However, there are two restrictions: (1) width of the rf bucket needs to be large enough, where $\Delta z_{bucket} = \lambda_{rf} \gg \sigma_z$; and (2) beam loading due to the rf-cavity impedance cannot be too large, where f_{BL} (=energy-loss per particle per eV_{rf}) is scaled approximately by $1/\lambda_{rf}^2$ [6]. For the cases we have examined we find that a S-band rf ($f_{rf} = 3\text{GHz}$) is a suitable candidate, compromising the requirements of a large V_{rf} slope, a large enough rf bucket width ($\Delta z_{sep} = 10\text{cm} \simeq 33\sigma_z$), and a small enough beam loading factor ($f_{BL} \approx 33\%$, obtained by numerical calculation of the energy loss of a Gaussian beam due to the rf cavity) [6]. Simulations show that one needs approximately 450 MeV of eV_{rf} for the 2 TeV machine and about 25 MeV for the 250 GeV machine to suppress the large excitations of bunch length and bunch energy spread. The requirement for large V_{rf}/λ_{rf} can, alternatively, be achieved by using two rf cavities. One cavity with higher frequency (X-band) provides large rf voltage gradient across the bunch (even if the cavity is overloaded), and the second cavity with lower frequency (S-band) supplies the beam energy lost due to interaction with impedance of the cavities and the ring [8]. Via this scheme, the total V_{rf} needed could perhaps be reduced. Detailed examination is underway.

1.3 Above or below transition? The sign of η_1 .

Simulations show that operation of the ring below transition $\eta_1 < 0$ produces less bunch-lengthening and energy-spreading than operation above transition $\eta_1 > 0$. A possible explanation is that when $\eta_1 < 0$ (> 0), the bunch tends to lean backward (forward) due to the potential-well distortion. The bunch tail thus experiences less (more) wake force generated by the bunch head. Consequently, the bunch tail lengthens less (more). Of course, this could depend on the impedance models, bunch length, and how bunch frequency spectrum overlaps with an impedance spectrum. Detailed discussions on the effect of negative η_1 can be found in Ref. [9].

1.4 Effects of longitudinal chromaticity: η_2 .

The longitudinal chromaticity η_2/η_1 introduces energy dependence into the synchrotron frequency in a way exactly analogous to the energy dependence of the betatron frequency described by transverse chromaticity. Similarly, the transverse head-tail instability due to the transverse chromaticity has a longitudinal counterpart - the longitudinal head-tail instability (LHT) driven by longitudinal chromaticity. The head-tail instabilities have no stability thresh-

old [10]. Moreover, when $\eta_2 \neq 0$, the rf-bucket is distorted and the phase space acceptance is reduced. The so called “ α -bucket” appears when η_2 is larger than some critical value. It is clear that the lattice design should have the value of η_2 minimized to avoid the LHT instability and reduction of longitudinal phase space acceptance.

1.5 Effects of nonlinear longitudinal chromaticity: η_3 .

It has been shown in a study of the transverse head-tail instability [11], that the nonlinear transverse chromaticity plays role similar to the varying transverse chromaticity (modulated by a synchrotron period), in which an otherwise accumulating head-tail phase is cancelled during the modulation. Similar to its transverse counterpart, the nonlinear longitudinal chromaticity η_3 , in contrasted to η_2 , does not cause the LHT instability but contributes an incoherent frequency spread that provides Landau damping. Our simulations show that, η_3 can help decrease energy-spreading of the bunch, when $\eta_1 \leq 10^{-6}$ and the synchrotron oscillation period is longer than the storage time.

1.6 Effects of beam-beam interaction

There are two longitudinal effects from the classical beam-beam interaction that could degrade the beam luminosity. The first is the hourglass effect for centered collisions, in which the luminosity decreases when σ_z grows at fixed β^* . This could occur when there is bunch lengthening due to microwave instability, or phase space mismatch. The second is the hourglass effect for longitudinally displaced collisions at the IP (Interaction Point). This could occur when there are bunch centroid shifts due to the potential-well distortion, rf phasing errors or injection timing errors [1]. Control of the bunch length and bunch centroid, described above, is therefore important to prevent these sources of luminosity degradation.

2 SCALING LAW FOR THE LONGITUDINAL STABILITY THRESHOLD

We examine the longitudinal behavior of 250 GeV \times 250 GeV and 2 TeV \times 2 TeV machines with a scaling law for the impedance threshold. The parameters essential to the scaling of the stability threshold are listed in Table 1. First we examine the scaling law for the energy spread (by using the low current matching condition):

$$\sigma_\delta = \sigma_z(\omega_s/c|\eta_1|) \propto \sigma_z \sqrt{(V_{rf}/\lambda_{rf})/(CE|\eta_1|)}. \quad (1)$$

According to Table 1, we have

$$\frac{\sigma_\delta(0.25\text{TeV})}{\sigma_\delta(2\text{TeV})} = 18.7 \sqrt{\frac{(V_{rf}/|\eta_1|\lambda_{rf})(0.25\text{TeV})}{(V_{rf}/|\eta_1|\lambda_{rf})(2\text{TeV})}}. \quad (2)$$

If we keep the same energy spread for both collider rings, then the rf needed is scaled as

$$\frac{V_{rf}/\lambda_{rf}(0.25\text{TeV})}{V_{rf}/\lambda_{rf}(2\text{TeV})} = \left(\frac{1}{350}\right) \left[\frac{|\eta_1|(0.25\text{TeV})}{|\eta_1|(2\text{TeV})}\right]. \quad (3)$$

The Boussard-modified Keil-Schnell criterion gives us the scaling law for the effective threshold-impedance [4], as $|Z_0^{\parallel}/n|_{the} \propto (E/e)|\eta_1|\sigma_\delta^2/I_p$. Since $I_p \propto N/\sigma_z$, we have

$$\frac{|Z_0^{\parallel}/n|_{the}(0.25\text{TeV})}{|Z_0^{\parallel}/n|_{the}(2\text{TeV})} = \frac{1}{6} \left[\frac{|\eta_1|(0.25\text{TeV})}{|\eta_1|(2\text{TeV})} \right]. \quad (4)$$

If we increase $|\eta_1|$ by a factor of 35 for the 250GeV machine, then V_{rf}/λ_{rf} needed (to satisfy the matching condition) becomes a factor of 10 smaller, and $|Z_0^{\parallel}/n|_{the}$ a factor of 5.83 larger. If the ring impedance of the low energy collider is below this threshold, then the wake voltage no longer dominates the longitudinal dynamics, and the matching condition needs to be approximately preserved. The scaling laws, from Eqs. (1) to (4), are thus self-consistent. Simulations show that the longitudinal behavior of the 250GeV machine is much easier to control.

3 CONCLUSION

Based on an estimate for the impedance and results of multi-particle simulations, we conclude that the longitudinal behavior in the Muon Collider rings can be controlled to a level that the luminosity will not be significantly degraded. The parameters for the rings are presented in Table 1. Results of simulation for the longitudinal behavior are shown in Figs. 1 and 2.

4 REFERENCES

- [1] $\mu^+\mu^-$ Collider: A Feasibility Study, BNL-52503, Fermi Lab-Conf.-96/92, LBNL-38946 (1996); $\mu^+\mu^-$ Colliders, Proc. of the Symposium on Physics Potential and Development of $\mu^+\mu^-$ Colliders, ed. D.B. Cline, Nuclear Physics B (Proc. Suppl.) 51A (1996).
- [2] W.-H.Cheng, A.M. Sessler, J.S. Wurtele and K.Y. Ng, Proceedings of the 5th European Particle Accelerator Conference, Barcelona, Vol. 2, p. 1081, June, 1996.
- [3] W.-H.Cheng, A.M. Sessler, and J.S. Wurtele, Lawrence Berkeley National Laboratory Report, LBNL-40224 (1997).
- [4] A. W. Chao, *Physics of Collective Beam Instabilities in High Energy Accelerators*, (John Wiley & Sons, 1993).
- [5] W. Turner, report in preparation, (1997).
- [6] P.B. Wilson, Stanford Linear Accelerator Center Report, SLAC-PUB-2884, (1982).
- [7] S. Krinsky and L.M. Wang, Part. Accel. **17**, 109 (1985).
- [8] Alvin Tollestrup, private communication, (1997).
- [9] S. X. Fang, *et al*, National Laboratory for High Energy Physics Report, Tsukuba-shi, KEK Preprint 94-190 (1995).
- [10] B. Chen and A. W. Chao, Particle Accelerators, vol. 43(1-2), pp. 77-91, 1993.
- [11] W.-H.Cheng, A.M. Sessler and J.S. Wurtele, Lawrence Berkeley National Laboratory Report, LBNL-39717 (1996).

Beam energy E (TeV)	2	0.25
Muons per bunch N (10^{12})	2	4
Circumference C (km)	8	1.3
Bunch length σ_z (cm)	0.3	0.8
Bunch energy spread σ_δ (%)	0.15	0.15
Slippage factor η_1 (10^{-6})	-2	-70
Longitudinal chromaticity η_2	0	0
Nonlinear long. chromaticity η_3	-0.1	-0.1
RF energy eV_{rf} (MeV/turn)	450	25
RF frequency f_{rf} (GHz)	3	3
RF phase-offset ϕ_{rf} (radian)	-0.32	-0.53
Synchrotron period $1/\nu_s$ (turn)	417.6	262.7

Table 1: Nominal parameters of the Collider Rings and the parameters for the rf and η used in simulations.

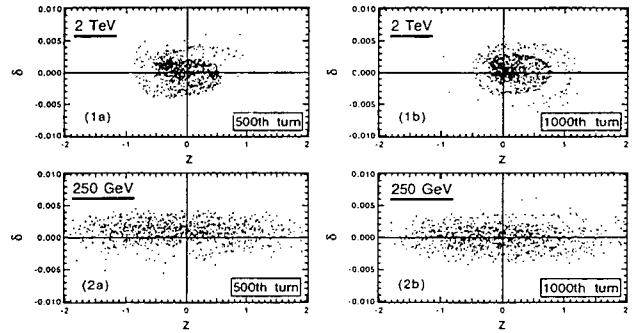


Figure 1: Multi-particle simulation results of the phase space in the (a) 500th and (b) 1000th turn, for the (1) 2 TeV ring and (2) 250 GeV ring. The initial distribution is bi-Gaussian in the phase space. The effect of mu-decay is included, the rf-cavity impedance and the impedances of a broad-band-resonator model are employed. Parameters used in simulations are shown in Table 1.

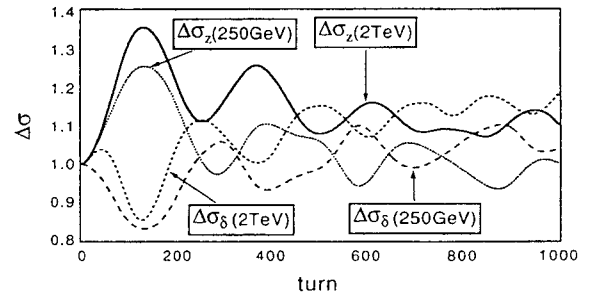


Figure 2: Simulation results of the excitation of bunch length and bunch energy spread for the 2 TeV ring and the 250 GeV ring, where $\Delta\sigma_z = \sigma_z/\sigma_z(0)$, $\Delta\sigma_\delta = \sigma_\delta/\sigma_\delta(0)$. Parameters used in simulations are shown in Table 1.